Drosophila attP40 background alters glomerular organization of the olfactory receptor neuron terminals

Qichen Duan[1], Rachel Estrella[1], Allison Carson[1], Yang Chen[1], Pelin C. Volkan[1, #]

[1]Department of Biology, Duke University, Durham, NC 27708

[#]Correspondence: pelin.volkan@duke.edu

Abstract

Bacteriophage integrase-directed insertion of transgenic constructs into specific genomic loci has been widely used by *Drosophila* community. A second chromosome-located *attP40* landing site gains popularity because of its high inducible expression levels of transgenes. Here, unexpectedly, we found that homozygous *attP40* chromosome leads to defects in the glomerular organization of Drosophila olfactory receptor neurons (ORNs). This effect is not likely to be caused by the loss of function of *Msp300*, where *attP40* docking site is inserted. Moreover, a*ttP40* site seems to genetically interact with a second chromosome *GAL4* driver, which also results in a similar ORN axon terminal defect. Though it remains elusive so far whether the ORN phenotype is caused by the neighboring genes around *Msp300* locus in the presence of *attP40*-based insertions or a second unknown mutation in the *attP40* background, our finding raises the critical issue with using this popular transgenic landing site. Rigorous controls are needed in the relevant experiments to rule out the *attP40*-associated background effects.

Introduction

RNA interference (RNAi)-based genetic screens provide scientists with powerful tools to identify genes involved in various biological processes (HOUSDEN *et al.* 2017). Binary expression systems, such as the *GAL4/UAS* system, induce the expression of various effectors in the desired cell populations (BRAND AND PERRIMON 1993). In Drosophila carrying transgenes for both cell-type-specific promoter-driven *GAL4* (driver) and *UAS-RNAi,* GAL4 protein binds *UAS* sites and drives RNAi expression, disrupting the expression and function of the target gene (BRAND AND PERRIMON 1993). As RNAi-based knockdown methods were becoming popular, efforts were initiated to make transgenic libraries of flies carrying *UAS-RNAi* targeting all the genes in the genome (DIETZL *et al.* 2007; NI *et al.* 2009; NI *et al.* 2011; PERKINS *et al.* 2015). These genome-wide libraries were then followed by efforts to generate thousands of *GAL4* lines that restrict expression to cellular subpopulations, enabling loss-of-function screens in cells of interest.

Among the RNAi collections, stocks from Transgenic RNAi Project (TRiP) have gained popularity because of their targeted integration of *UAS-RNAi* transgenes into the genome, efficient expression induced by appropriate *GAL4* drivers in different tissues, and high specificity with minimal expected off-target effects (MARKSTEIN *et al.* 2008; NI

et al. 2008; PERKINS *et al.* 2015). To expedite the generation of transgenic libraries, two predetermined chromosomal docking sites were targeted for recombination events that insert *UAS-RNAi* transgenes: *attP40* on the second chromosome and *attP2* on the third chromosome (MARKSTEIN *et al.* 2008). With the presence of bacteriophage-originated phiC31 integrase (by co-injection of integrase mRNA or germline-expressing transgenic integrase), the *UAS-RNAi* construct can be inserted into the corresponding docking sites (GROTH *et al.* 2004; NI *et al.* 2008). *AttP40* and *attP2* sites are selected because they exhibit optimal inducible expression levels upon binding with diverse tissue-specific *GAL4* drivers (MARKSTEIN *et al.* 2008). Therefore, in addition to the TRiP *UAS-RNAi* library, many other transgenes, including tissue-specific drivers (*GAL4*, *QF*, *LexA*) and *UAS/QUAS/LexAop-effectors/reporters* are also routinely integrated into these two landing sites (ZIRIN *et al.* 2020).

Given the widespread use of transgenic flies with *attP40* and *attP2* backbones, we must be more cognizant of possible genetic background effects during phenotypic analysis. Both *attP40* and *attP2* docking sites are in chromosomal regions populated by many genes. These sites, like any insertion into the genome, can disrupt function of nearby genes. More specifically, *attP40* site is located within one of the large introns of *Msp300* gene while *attP2* site is inserted in the 5' untranslated region (UTR) of *Mocs1* gene (LARKIN *et al.* 2020). Both Msp300 and Mocs1 have critical biological roles. Specifically, Msp300 is the *Drosophila melanogaster* orthologue of mammalian Nesprins, which organize postsynaptic cytoskeleton scaffold and are required for stabilization of new synapses (ELHANANY-TAMIR *et al.* 2012; MOREL *et al.* 2014; TITLOW *et al.* 2020; ZHENG *et al.* 2020). Mocs1 is involved in Mo-molybdopterin cofactor biosynthetic process and inter-male aggressive behaviors (GAUDET *et al.* 2011; RAMIN *et al.* 2019). It is unclear how the insertion of various transgenic constructs into *attP40* and *attP2* docking sites would affect the function of these host genes which may further result in phenotypic defects.

Indeed, recent studies have raised issues related to landing site-associated effects. For example, van der Graaf et al. showed flies bearing two copies of *attP40*-derived insertions also show decreased *Msp300* transcript levels (VAN DER GRAAF *et al.* 2022). In addition, this study also reported defects in muscle nuclei spacing in larval stages in the *attP40* homozygous background, which phenocopies *Msp300* mutants (VAN DER GRAAF *et al.* 2022). These results suggest that *attP40* docking site and *attP40*-based transgenes are insertional mutations of *Msp300* gene (VAN DER GRAAF *et al.* 2022). Another study reported that *attP40* flies show resistance to cisplatin-induced neuronal damage, compared to *attP2* background (GROEN *et al.* 2022). This study tied the effect to the reduced *ND-13A* (NADH dehydrogenase 13 kDA subunit, a component of mitochondrial complex I) expression in *attP40* homozygous flies (GROEN *et al.* 2022). It is noteworthy that *ND-13A* flanks the 5' UTR of *Msp300* and is downstream of *attP40* docking site. Together, these results imply the integration of *attP40* docking site significantly changes the local transcriptional state and interferes with the transcription of surrounding genes.

During a GAL4-driven *UAS-RNAi* screen for olfactory neuron axon organization, we observed an axon terminal phenotype that is associated with *attP40* background. The phenotype occurs in the flies homozygous for *attP40* docking site alone or with various

transgenic insertions, independent of the identity of the transgene. Notably, the phenotype observed in *attP40* background appears to be recessive but is independent of *Msp300* function, possibly implicating other *attP40* background mutations nearby or in other locations on the second chromosome. Though the nature of the mutation is unclear, the background effects should be mitigated by designing more rigorous controls to interpret phenotypic data obtained using reagents in concert with *attP40* backgrounds.

Materials and methods

Drosophila stocks and genetics

Drosophila were raised in classic molasses media provided by Archon Scientific. For the RNAi screen experiments, flies were raised at 28 °C to maximize the knockdown efficiency. Most of the other crosses were also kept at 28 °C, except for the experiments shown in Figure 1F, which were conducted at room temperature (23 °C). After eclosion, the flies are aged for 5-7 days before dissection. In addition to the *UAS-RNAi* stocks from Bloomington Drosophila Stock Center (listed in Figure 1B), the following stocks are used: *UAS-RFP RNAi attP2* (BDSC# 35785), *UAS-beat-Ia RNAi* GD1386 (VDRC# 4544), *attP40* (BDSC# 36304), *attP2* (BDSC# 36303), *ctrl-gRNA attP40* (BDSC# 67539), *UAS-RFP attP40* (BDSC# 32222), $Msp300^{deltaKASH}$ (BDSC# 26781), $Msp300^{MI01145}$ (BDSC# 53050), $Msp300^{MI00111}$ (BDSC# 30623), $Msp300^{KG03631}$ (BDSC# 13024); *Or47b-GAL4* (chr2), *Or47b-GAL4* (chr3), *Or43a-GAL4* (chr2), *Or47a-GAL4* (chr2) (VOSSHALL *et al.* 2000; FISHILEVICH AND VOSSHALL 2005), and *Gr21a-GAL4* (chr2) (SCOTT *et al.* 2001)) are gifts from Dr. Leslie Vosshall; *UAS-SytGFP* (chr2 or chr3) is a Volkan lab stock (BARISH *et al.* 2018). The line *Or47b-GAL4, Or47a-GAL4, Or43a-GAL4, Gr21a-GAL4, UAS-SytGFP/CyO* was recombined and balanced from the above components.

Immunocytochemistry

Flies were sacrificed in 70% ethanol. Fly brains were then dissected in PBST buffer (0.2% Triton X-100 in 1X PBS), fixed in 4% paraformaldehyde for 30 mins, followed by washing with PBST for three 10-min cycles. Brains were incubated in the primary antibody mix at 4 °C overnight, followed by three 20-min washes with PBST at room temperature, then incubated in the secondary antibody mix at 4 °C overnight. The brains were washed again by three 20-min wash with PBST before being mounted on the slide for imaging. The blocking was done together with each antibody incubation, with 1% natural goat serum mixed with primary and secondary antibodies, respectively. The following primary antibodies were used: 1:1000 rabbit anti-GFP (Invitrogen), 1:20 rat anti-Ncad (DSHB); the following secondary antibodies were used: 1:1000 Alexa Fluor 488 goat anti-rabbit IgG (Invitrogen), 1:200 Alexa Fluor 647 goat anti-rat IgG (Invitrogen); all antibodies are diluted in PBST.

Confocal imaging and phenotypic quantification

Confocal imaging was performed by either Olympus Fluoview FV1000 microscope or Zeiss 880 microscope. Brains were imaged across Z-axis from the posterior side to the most anterior side of the antennal lobes, and all confocal sections were overlayed for phenotypical analysis. The same set of imaging parameters was used between experimental and control groups. The phenotype was qualitatively determined by glomerular morphology, i.e., whether Or47b ORN axons appear in the dorsal antennal lobe region, in contrast to the typical V-shaped glomerulus in wild-type controls. The phenotype shown in Figure 1 (glomerular expansion) is largely consistent from brain to brain, while the phenotypes shown in Figure 2B,E exhibit variability, which were categorized into expansion or dorsal shift. The phenotype was quantified by the percentage of antennal lobes exhibiting each defect among all the brains examined in respective groups. P-value was calculated by two-tailed Fisher's exact test through the built-in functions of GraphPad Prism 9 software.

Results

We used the *Drosophila* olfactory receptor neurons (ORNs) as a model to understand the molecular mechanisms underlying neuronal circuit assembly. In *Drosophila*, each class of ORNs expresses a unique olfactory receptor (*Or*) gene, and ORN axons target to the brain antennal lobe within class-specific and uniquely positioned synaptic units called glomeruli (HONG AND LUO 2014; BARISH AND VOLKAN 2015). To identify the molecular players contributing to the glomerular organization of the ORNs, we genetically screened genes encoding cell adhesion molecules whose expression levels increase over pupal development in the antennae (BARISH *et al.* 2018). Among these, *beat* and *side* gene families drew our attention because they encode the Ig superfamily proteins, form a heterophilic interacting protein network, and have been previously revealed to be involved in neuronal adhesion (FAMBROUGH AND GOODMAN 1996; PIPES *et al.* 2001; SINK *et al.* 2001; DE JONG *et al.* 2005; SIEBERT *et al.* 2009; ÖZKAN *et al.* 2013; LI *et al.* 2017; KINOLD *et al.* 2021). We obtained a collection of transgenic *UAS-RNAi* lines from TRiP library deposited at the Bloomington Drosophila Stock Center (BDSC) and crossed these lines with an established recombinant chromosome containing four different *Or* promoter-driven *GAL4* transgenes (*Or47a-GAL4*, *Or47b-GAL4*, *Or23a-GAL4*, *Gr21a-GAL4*) together with a *UAS-SytGFP* reporter. We examined the knockdown effect of candidate genes on axonal targeting of these four ORN classes. The parent flies with a single copy of the *GAL4* drivers showed wild type glomerular organization (Figure 1A). As an additional control, we also crossed *GAL4* driver lines to flies expressing the RNAi against a red fluorescent protein (RFP) mCherry, which also exhibited no apparent defect in glomerular organization (Figure 1A).

From the screen, we found a strikingly recurrent phenotype, where the axon terminals of Or47b ORNs invade the neighboring region, leading to an expanded round VA1v glomerulus in contrast to the crescent shape in control brains (Figure 1A). This phenotype was observed in two independent RNAi lines targeting the same gene, for example, *beat-Ia* (Figure 1A). However, screening a list of *beat* and *side* family

members revealed a pattern for the phenotype, which only correlated with the second chromosome *UAS-RNAi* transgenes, independent of the gene identity. Figure 1B summarizes the screening results from *beat/side* gene families. All the RNAi lines inserted at the second chromosome *attP40* site yielded the expanded VA1v glomerulus phenotype, whereas none of the RNAi lines inserted at the third chromosome *attP2* site showed this defect. Notably, there is one gene, *beat-IIIc*, with one *attP40*-derived RNAi line and one *attP2*-derived RNAi line. Only the *attP40 UAS-RNAi* insertion gave rise to the phenotype (Figure 1B). The same phenotype was also observed with randomly selected TRiP *UAS-RNAi* lines inserted at the *attP40* site targeting genes without known roles in ORN development (data not shown). To test whether this phenotype is caused by specific effects of RNAi-mediated gene knockdown or simply by the presence of *attP40*-derived insertions, we first crossed the same *Or47b-GAL4* driver line to a third GD *UAS-RNAi* line from Vienna Drosophila Resource Center (VDRC) targeting *beat-Ia*, which was generated by random P-element mediated insertions (DIETZL *et al.* 2007). The GD *UAS-RNAi* line could not reproduce the phenotype obtained by the *attP40*-derived *UAS-RNAi* from the TRiP collection (Figure 1C). In addition, crossing the driver line to an empty *attP40* site without any transgenes led to the same glomerular expansion phenotype (Figure 1D). These results suggest that the Or47b ORN-specific VA1v glomerular defect is independent of the RNAi-based knockdown of the genes examined but caused by an effect from the *attP40*-derived chromosome.

Since we repeatedly obtained the VA1v glomerular phenotype with the second chromosome *Or47b-GAL4*-driven *UAS-RNAi*, we also tested if crossing flies carrying the same *Or47b-GAL4* transgene to various *attP40* derivatives could result in the same phenotype (Figure 1E). Compared with the no *attP40* control (over a *CyO* balancer chromosome), the *attP40* landing site with and without *UAS-RNAi* insertion, *UAS-RFP*, or a ubiquitous promoter-driven gRNA targeting the *QUAS* sequence (control gRNA) all produced the same VA1v glomerular defect when crossed to the second chromosome *Or47b-GAL4*-driven *UAS-SytGFP* (Figure 1F). This phenotype is not due to the dominant effect of *attP40* or *attP40* derivatives, as animals with a single copy of *attP40*-derived insertion with a third chromosome-located *Or47b-GAL4* driver appeared wild type (Figure 1G,H). Only the combination of the second chromosome *Or47b-GAL4* over the *attP40* docking site or *attP40* derivatives yielded the glomerular targeting defects. This result suggests that *attP40* chromosome genetically interacts with the second chromosome *Or47b-GAL4* driver background to generate the VA1v glomerular defect.

Surprisingly, homozygous *attP40* derivatives or *attP40* empty docking site alone could produce similar axon terminal defects when a third chromosome *Or47b-GAL4 UAS-sytGFP* transgenes were used. Flies heterozygous for *attP40* site with or without transgenes appeared wild type (Figure 2A-F). Most of the brains in flies homozygous for *attP40* site with or without insertions displayed a dorsally positioned VA1v glomerulus (Figure 2B,E, middle panels; Figure 2C,F), whereas a small proportion also exhibited an expanded glomerulus (Figure 2B,E, right panels; Figure 2C,F). Given that *attP40* site is located within an intron of *Msp300* gene, we posited that it likely disrupts *Msp300* function. *Msp300* encodes a Nesprin-like protein, which is required for proper positioning of muscle nuclei and neuromuscular junction formation (ELHANANY-TAMIR *et al.* 2012; MOREL *et al.* 2014). Single-cell RNA-seq datasets from ORNs also show broad

expression of *Msp300* across ORN classes (LI *et al.* 2022). We thus tested if the VA1v glomerular defect is caused by the loss of *Msp300* function. We analyzed transheterozygotes of empty *attP40* docking site over other mutant alleles of *Msp300*, such as *Msp300*^{deltaKASH} (which lacks the KASH domain (XIE AND FISCHER 2008; ELHANANY-TAMIR *et al.* 2012)), *Msp300*^{MI00111}, *Msp300*^{MI01145} (two MIMIC-based alleles predicted to disrupt most splice isoforms of *Msp300* transcripts (VENKEN *et al.* 2011)), and *Msp300*^{KG03631} (a P-element-based insertion which is close to *attP40* landing site (BELLEN *et al.* 2004)) (Figure 2G). However, none of these genetic combinations produced the same VA1v glomerular phenotype (Figure 2H). This indicates that the VA1v glomerular defect is independent of the *Msp300* function and is likely caused by a second recessive mutation linked to the *attP40* docking site.

Figure 1

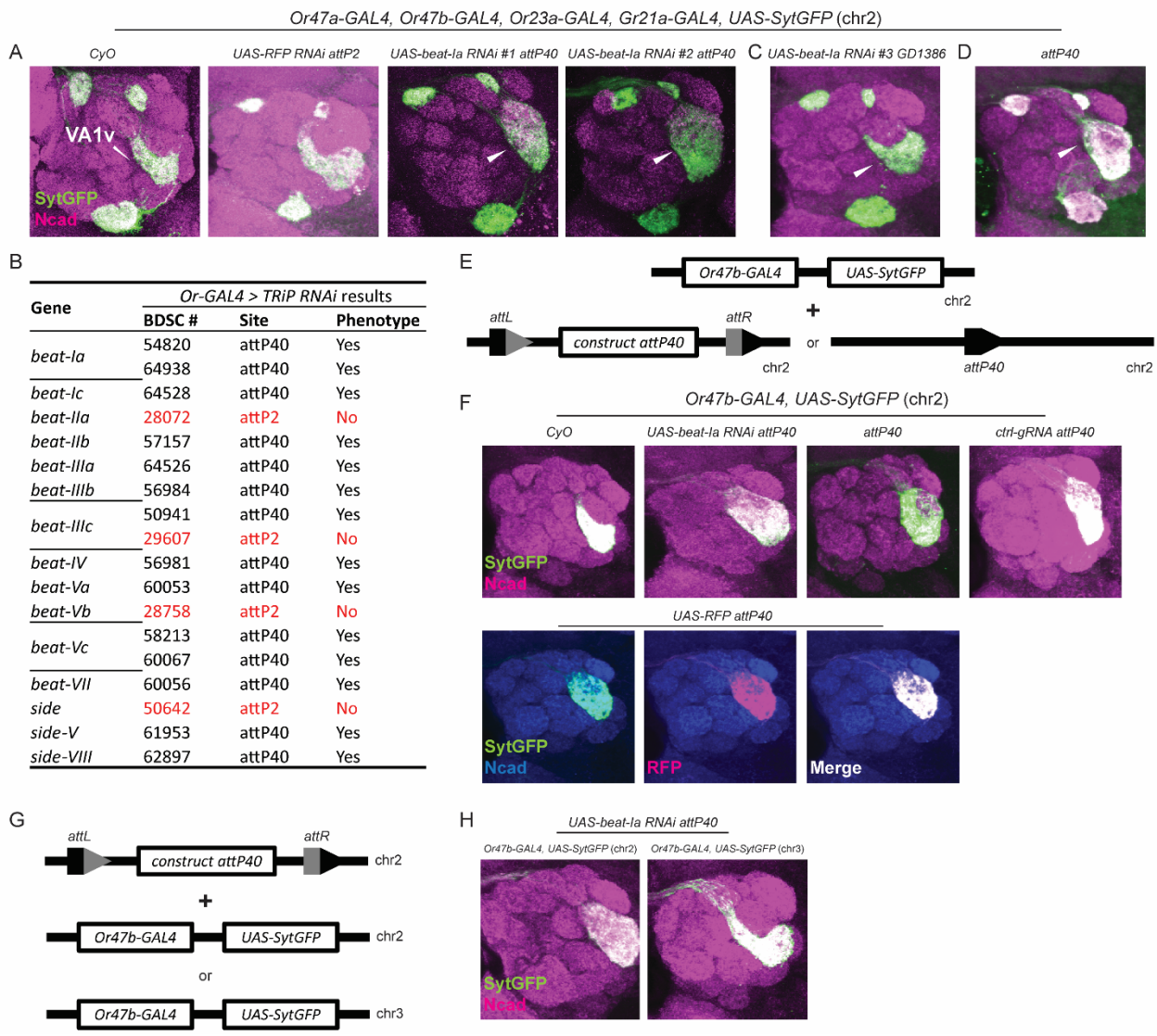

Figure 1. Drosophila *attP40* site genetically interacts with a second chromosome *Or47b-GAL4* background resulting in glomerular defects. (A, C & D) Confocal images of representative brains from a genetic screen to identify adhesion molecules involved in the glomerular organization of the Drosophila olfactory receptor neuron axon terminals. We crossed a second chromosome containing four different Drosophila olfactory receptor promoter-driven *GAL4s (Or47a-, Or47b-, Or23a-, Gr21a-)* together with a *UAS-SytGFP* reporter to the indicated *UAS-RNAi* lines or *attP40* background flies. The parental driver chromosome over the *CyO* balancer was used as a no-RNAi control. The invading Or47b ORN axons are denoted with white arrowheads. (B) Summary of the phenotypical results from the genetic screen focusing on *beat/side* gene families. The Bloomington stock number and the transgenic docking site of each line are also listed. (E, F) Schematic in (E) shows the genotype of animals used in (F), where each fly has one copy of the second chromosome carrying an *Or47b-GAL4* driver and a *UAS-SytGFP* reporter, and one copy of the indicated second chromosome, either a *CyO* balancer or *attP40* docking site derivatives. *attL* and *attR* sites are generated as a result of transgene integration into *attP40* docking site. Confocal images of representative brains are shown in F. (G, H) Schematic in G shows the genotype of animals used in (H), where each fly has one copy of the second chromosome *UAS-beat-Ia RNAi* transgene inserted into the *attP40* docking site, with *Or47b-GAL4* driver and a *UAS-SytGFP* reporter, either on the second or third chromosome. Confocal images of representative brains are shown in (H). 10~25 brains were examined in each genotype and the phenotypical penetrance is almost 100% in each condition.

Figure 2

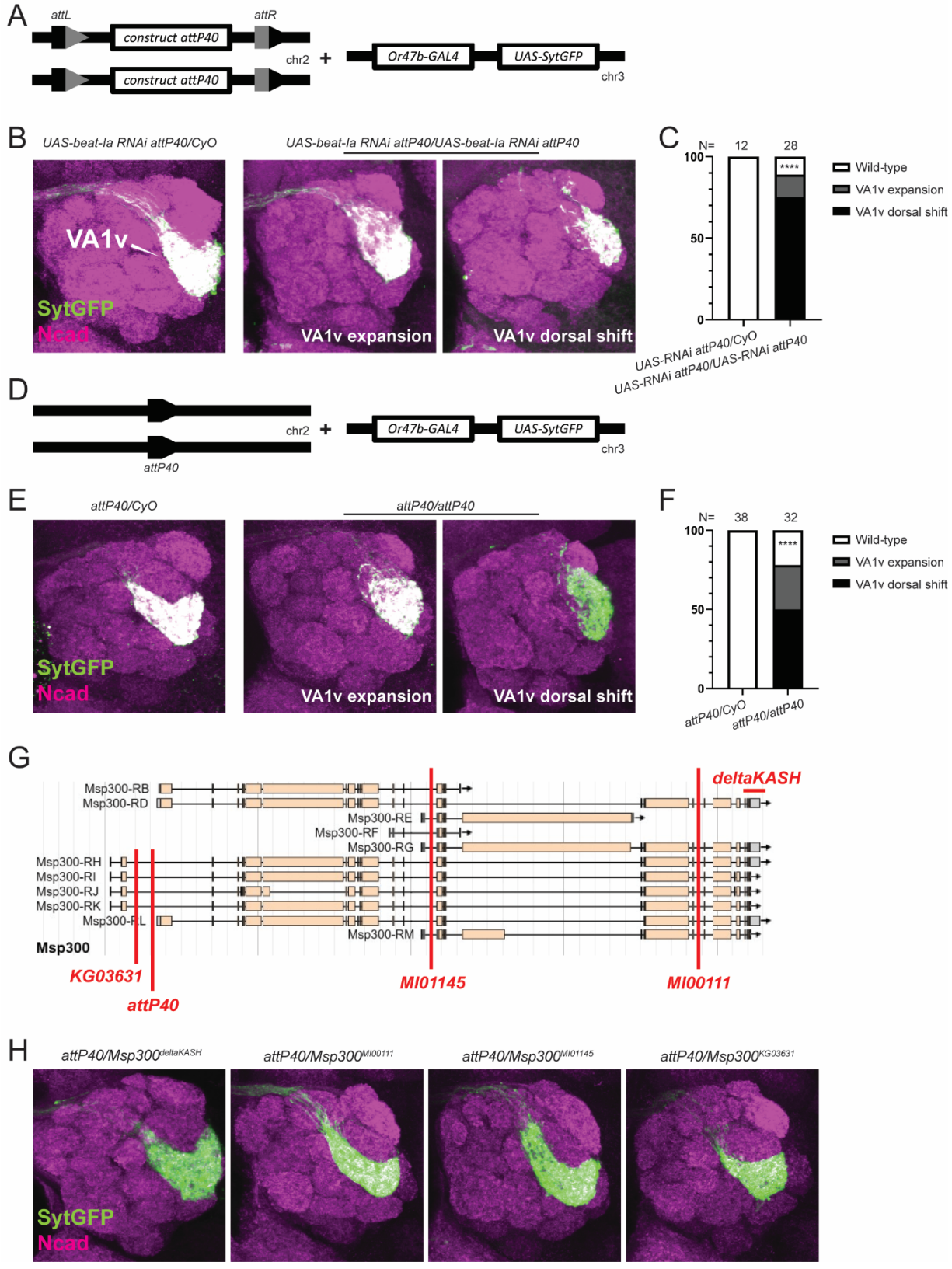

251

Figure 2. Homozygous *attP40* chromosome affects glomerular organization independent of the *Msp300* function. (A-C) Schematic in (A) shows the genotype of animals used in (B), where each fly has one or two copies of the second chromosome *UAS-beat-Ia RNAi* transgene inserted at the *attP40* docking site, with the third chromosome *Or47b-GAL4 UAS-SytGFP* transgenes. Confocal images of representative brains are shown in (B). The percentage of the phenotypes is shown in (C). ****, p<0.0001 after Fisher's exact test. (D-F) Schematic in (D) shows the genotype of animals used in (E), where each fly has one or two copies of the second chromosome empty *attP40* docking site, with the third chromosome *Or47b-GAL4 UAS-SytGFP* transgenes. Confocal images *of* representative brains are shown in (D). The percentage of the phenotypes is shown in (F). ****, p<0.0001 after Fisher's exact test. N in (C) and (F) denotes the antennal lobes examined. (G) Schematic showing the *Msp300* genomic locus, the *attP40* docking site, three insertional *Msp300* mutations ($Msp300^{MI00111}$, $Msp300^{MI01145}$, $Msp300^{KG03631}$), and one deletion allele ($Msp300^{deltaKASH}$), each denoted with red lines. (H) Confocal images of representative brains of the indicated transheterozygous animals, with *attP40* docking site over the indicated *Msp300* alleles. N = 11, 8, 4, 12 brains in each genotype group, from left to right.

Discussion

Here, we found that homozygous *attP40* chromosome leads to defective glomerular organization of ORNs. This defect is likely not caused by the loss of *Msp300* function, where *attP40* site is inserted. Moreover, a*ttP40* site genetically interacts with a second chromosome carrying the *Or47b-GAL4* transgene, resulting in a similar ORN axon terminal defect. Though the exact genetic reasons and molecular mechanisms are unknown, our finding raises the critical issue with using this popular transgene landing site. Rigorous controls are needed to rule out the *attP40*-associated background effects.

A recent study reported that flies homozygous for *attP40*-derived insertions had 50% reduction in *Msp300* transcript levels and phenocopied the defects in larval muscle nuclei clustering in *Msp300* mutants (VAN DER GRAAF *et al.* 2022). As homozygotes of the *attP40* chromosome are defective in Or47b ORN axon terminal organization, we hypothesized that the *attP40*-affected *Msp300* gene is responsible for the defect. However, this is not the case as *attP40* over various *Msp300* mutations appeared phenotypically wild type, suggesting *attP40* chromosome may carry an unannotated mutation. Further support for this comes from the normal *Msp300* transcript levels in flies homozygous for empty *attP40* docking site despite exhibiting defective muscle nuclei spacing (VAN DER GRAAF *et al.* 2022). Thus, it is possible that *attP40* docking site generates either a weak hypomorphic mutation in *Msp300* that does not drastically alter transcript levels, or that the observed nuclei phenotype in *attP40* homozygotes is independent of *Msp300*. Additional loss-of-function or rescue experiments are needed to distinguish between these possibilities.

The *attP40* docking site with or without transgene insertions may also disrupt other genes in the vicinity of *Msp300*. For example, in addition to *Msp300, attP40* docking site is flanked on the opposing side by *ND-13A,* which encodes a component of the

mitochondria electron transport chain complex I. Thus, *attP40* docking site alone or transgene insertions may lead to a variety of phenotypes as a result of disrupted *ND-13A*. Indeed, Groen et al. reported that *attP40* flies exhibit resistance to cisplatin-induced neuronal damage mediated by the reduced expression of *ND-13A* (GROEN *et al.* 2022). Whether the glomerular defect is dependent on the *ND-13A* function is beyond the scope of this paper but needs to be test in the future studies.

Surprisingly, we found transheterozygous animals with an *attP40* chromosome over the second chromosome *Or47b-GAL4* transgene produced similar glomerular abnormalities. This suggests that the second chromosome bearing *Or47b-GAL4* driver may carry similar background mutations as the *attP40* chromosome. Nevertheless, since the *Or47b-GAL4/attP40* phenotype is not qualitatively identical to the *attP40/attP40* one, another possibility is that these two chromosomes possess alleles of two different genes that interact with each other in the same genetic pathway.

To summarize, we found unexpected background effects of *Drosophila attP40* landing site on the ORN glomerular organization. In parallel with other recent studies reporting other phenotypes arising from the *attP40* background, ranging from muscle development to neuronal stress responses, such background effects should be seriously considered in using *attP40*-derived flies. It is recommended to avoid using homozygotes/double-copies of the *attP40*-based insertions. Researchers should also be aware of the potential genetic interactions between the *attP40*-bearing chromosome and the other homologous second chromosomes even if it doesn't contain any *attP40* derivatives. Appropriate controls should be applied to override these caveats. For example, when working with *GAL4/UAS-effector* binary system, it is better to use a GAL4-driven *UAS-neutral effector* (such as a scrambled RNAi inserted at the same docking site) as a negative control, rather than the widespread use of *GAL4* alone or *UAS-effector* alone controls. Transgenic rescue of RNAi-based gene knockdowns is not feasible due to targeting of rescue transgenes by the RNAi. Thus, use of full animal mutants or MARCM based clonal mutant analysis should be coupled with RNAi-based phenotypic analyses. Though the underlying genetic reasons remain elusive, studies demonstrated that the *attP40* landing site on chromosome II affects the expression of multiple genes (GROEN *et al.* 2022; VAN DER GRAAF *et al.* 2022). Additional omics-based experiments in the future will be needed to determine all the genetic lesions in the *attP40* strain that underly many phenotypic defects observed in this background. These studies will also reveal potential genetic alterations associated with glomerular defects, providing new insights into ORN axon pathfinding and glomerular organization.

Data availability

The authors affirm that all the data necessary for drawing the conclusions are present in the text, figures, and figure legends. Most of the *Drosophila* stocks are obtained from Bloomington or Vienna stock center, with identifiers listed in the materials and methods section. All the other lines are available upon request.

Acknowledgments

We would like to thank Bloomington Drosophila Stock Center and Vienna Drosophila Resource Center for providing all the fly stocks. We thank Duke Light Microscopy Core Facility for help with imaging.

Funding

This study is funded by grant NSF 2006471 and NIH 5R01NS109401 (both to P.C.V.). Q.D. is supported by Duke Biology Department Ph.D. program.

Conflicts of interest

The authors declare no conflict of interest with the contents of this paper.

Author contribution

Q.D. and P.C.V. conceived the study and designed the experiments; Q.D. did most of the experiments with help from R.E., A.C., and Y.C.; Q.D. analyzed the data and prepared the figures; Q.D. and P.C.V. wrote and edited the manuscript.

References

Barish, S., S. Nuss, I. Strunilin, S. Bao, S. Mukherjee *et al.*, 2018 Combinations of DIPs and Dprs control organization of olfactory receptor neuron terminals in Drosophila. PLoS Genet 14**:** e1007560.

Barish, S., and P. C. Volkan, 2015 Mechanisms of olfactory receptor neuron specification in Drosophila. Wiley Interdiscip Rev Dev Biol 4**:** 609-621.

Bellen, H. J., R. W. Levis, G. Liao, Y. He, J. W. Carlson *et al.*, 2004 The BDGP Gene Disruption Project: Single Transposon Insertions Associated With 40% of Drosophila Genes. Genetics 167**:** 761-781.

Brand, A. H., and N. Perrimon, 1993 Targeted gene expression as a means of altering cell fates and generating dominant phenotypes. Development 118**:** 401-415.

de Jong, S., J. A. Cavallo, C. D. Rios, H. A. Dworak and H. Sink, 2005 Target recognition and synaptogenesis by motor axons: responses to the sidestep protein. Int J Dev Neurosci 23**:** 397-410.

Dietzl, G., D. Chen, F. Schnorrer, K.-C. Su, Y. Barinova *et al.*, 2007 A genome-wide transgenic RNAi library for conditional gene inactivation in Drosophila. Nature 448**:** 151-156.

Elhanany-Tamir, H., Y. X. V. Yu, M. Shnayder, A. Jain, M. Welte *et al.*, 2012 Organelle positioning in muscles requires cooperation between two KASH proteins and microtubules. Journal of Cell Biology 198**:** 833-846.

Fambrough, D., and C. S. Goodman, 1996 The Drosophila beaten path gene encodes a novel secreted protein that regulates defasciculation at motor axon choice points. Cell 87**:** 1049-1058.

Fishilevich, E., and L. B. Vosshall, 2005 Genetic and functional subdivision of the Drosophila antennal lobe. Curr Biol 15**:** 1548-1553.

Gaudet, P., M. S. Livstone, S. E. Lewis and P. D. Thomas, 2011 Phylogenetic-based propagation of functional annotations within the Gene Ontology consortium. Brief Bioinform 12**:** 449-462.

Groen, C. M., J. L. Podratz, J. Pathoulas, N. Staff and A. J. Windebank, 2022 Genetic Reduction of Mitochondria Complex I Subunits is Protective against Cisplatin-Induced Neurotoxicity in Drosophila. Journal of Neuroscience 42**:** 922-937.

Groth, A. C., M. Fish, R. Nusse and M. P. Calos, 2004 Construction of transgenic Drosophila by using the site-specific integrase from phage ϕC31. Genetics 166**:** 1775-1782.

Hong, W., and L. Luo, 2014 Genetic control of wiring specificity in the fly olfactory system. Genetics 196**:** 17-29.

Housden, B. E., M. Muhar, M. Gemberling, C. A. Gersbach, D. Y. Stainier *et al.*, 2017 Loss-of-function genetic tools for animal models: cross-species and cross-platform differences. Nature Reviews Genetics 18**:** 24-40.

Kinold, J. C., M. Brenner and H. Aberle, 2021 Misregulation of Drosophila Sidestep Leads to Uncontrolled Wiring of the Adult Neuromuscular System and Severe Locomotion Defects. Front Neural Circuits 15**:** 658791.

Larkin, A., S. J. Marygold, G. Antonazzo, H. Attrill, G. dos Santos *et al.*, 2020 FlyBase: updates to the Drosophila melanogaster knowledge base. Nucleic Acids Research 49**:** D899-D907.

Li, H., J. Janssens, M. De Waegeneer, S. S. Kolluru, K. Davie *et al.*, 2022 Fly Cell Atlas: A single-nucleus transcriptomic atlas of the adult fruit fly. Science 375**:** eabk2432.

Li, H., A. Watson, A. Olechwier, M. Anaya, S. K. Sorooshyari *et al.*, 2017 Deconstruction of the beaten Path-Sidestep interaction network provides insights into neuromuscular system development. Elife 6.

Markstein, M., C. Pitsouli, C. Villalta, S. E. Celniker and N. Perrimon, 2008 Exploiting position effects and the gypsy retrovirus insulator to engineer precisely expressed transgenes. Nature genetics 40**:** 476-483.

Morel, V., S. Lepicard, A. N Rey, M.-L. Parmentier and L. Schaeffer, 2014 Drosophila Nesprin-1 controls glutamate receptor density at neuromuscular junctions. Cellular and molecular life sciences 71**:** 3363-3379.

Ni, J.-Q., L.-P. Liu, R. Binari, R. Hardy, H.-S. Shim *et al.*, 2009 A Drosophila resource of transgenic RNAi lines for neurogenetics. Genetics 182**:** 1089-1100.

Ni, J.-Q., M. Markstein, R. Binari, B. Pfeiffer, L.-P. Liu *et al.*, 2008 Vector and parameters for targeted transgenic RNA interference in Drosophila melanogaster. Nature methods 5**:** 49-51.

Ni, J.-Q., R. Zhou, B. Czech, L.-P. Liu, L. Holderbaum *et al.*, 2011 A genome-scale shRNA resource for transgenic RNAi in Drosophila. Nature methods 8**:** 405-407.

Özkan, E., R. A. Carrillo, C. L. Eastman, R. Weiszmann, D. Waghray *et al.*, 2013 An extracellular interactome of immunoglobulin and LRR proteins reveals receptor-ligand networks. Cell 154**:** 228-239.

Perkins, L. A., L. Holderbaum, R. Tao, Y. Hu, R. Sopko *et al.*, 2015 The transgenic RNAi project at Harvard Medical School: resources and validation. Genetics 201**:** 843-852.

Pipes, G. C., Q. Lin, S. E. Riley and C. S. Goodman, 2001 The Beat generation: a multigene family encoding IgSF proteins related to the Beat axon guidance molecule in Drosophila. Development 128**:** 4545-4552.

Ramin, M., Y. Li, W. T. Chang, H. Shaw and Y. Rao, 2019 The peacefulness gene promotes aggression in Drosophila. Mol Brain 12**:** 1.

Scott, K., R. Brady, Jr., A. Cravchik, P. Morozov, A. Rzhetsky *et al.*, 2001 A chemosensory gene family encoding candidate gustatory and olfactory receptors in Drosophila. Cell 104**:** 661-673.

Siebert, M., D. Banovic, B. Goellner and H. Aberle, 2009 Drosophila motor axons recognize and follow a Sidestep-labeled substrate pathway to reach their target fields. Genes Dev 23**:** 1052-1062.

Sink, H., E. J. Rehm, L. Richstone, Y. M. Bulls and C. S. Goodman, 2001 sidestep encodes a target-derived attractant essential for motor axon guidance in Drosophila. Cell 105**:** 57-67.

Titlow, J., F. Robertson, A. Järvelin, D. Ish-Horowicz, C. Smith *et al.*, 2020 Syncrip/hnRNP Q is required for activity-induced Msp300/Nesprin-1 expression and new synapse formation. Journal of Cell Biology 219.

van der Graaf, K., S. Srivastav, P. Singh, J. A. McNew and M. Stern, 2022 The Drosophila attP40 docking site and derivatives are insertion mutations of MSP300. bioRxiv.

Venken, K. J., K. L. Schulze, N. A. Haelterman, H. Pan, Y. He *et al.*, 2011 MiMIC: a highly versatile transposon insertion resource for engineering Drosophila melanogaster genes. Nat Methods 8**:** 737-743.

Vosshall, L. B., A. M. Wong and R. Axel, 2000 An olfactory sensory map in the fly brain. Cell 102**:** 147-159.

Xie, X., and J. A. Fischer, 2008 On the roles of the Drosophila KASH domain proteins Msp-300 and Klarsicht. Fly 2**:** 74-81.

Zheng, Y., R. A. Buchwalter, C. Zheng, E. M. Wight, J. V. Chen *et al.*, 2020 A perinuclear microtubule-organizing centre controls nuclear positioning and basement membrane secretion. Nature cell biology 22**:** 297-309.

Zirin, J., Y. Hu, L. Liu, D. Yang-Zhou, R. Colbeth *et al.*, 2020 Large-Scale Transgenic Drosophila Resource Collections for Loss- and Gain-of-Function Studies. Genetics 214**:** 755-767.